

Experimental and theoretical elastic cross sections for electron collisions with the C₃H₆ isomers

C. Makochekanwa^{a)}*Physics Department, Sophia University, Chiyoda-ku, Tokyo 102-8554, Japan and Graduate School of Sciences, Kyushu University, Fukuoka 812-8581, Japan*

H. Kato, M. Hoshino, and H. Tanaka

Physics Department, Sophia University, Chiyoda-ku, Tokyo 102-8554, Japan

H. Kubo

Naka Fusion Research Establishment, Japan Atomic Energy Research Institute, Ibaraki-ken 311-019, Japan

M. H. F. Bettega

Departamento de Fisica, Universidade Federal do Parana, Caixa Postal 19044, Curitiba, Parana 81531-990, Brazil

A. R. Lopes, M. A. P. Lima, and L. G. Ferreira

Instituto de Fisica Gleb Wataghin, Universidade Estadual de Campinas, Campinas, Sao Paulo 13083-970, Brazil

(Received 2 September 2005; accepted 4 November 2005; published online 12 January 2006)

In the present work we report cross sections for electron collisions with the isomers propene (C₃H₆) and cyclopropane (*c*-C₃H₆). Electron-scattering differential cross sections (DCS) are reported for measurements carried out for energies 1.5–100 eV and the angular range of 20°–120°. Elastic integral cross sections (ECS), DCS, and momentum-transfer cross sections (MTCS) are reported for calculations carried out using the Schwinger multichannel method with pseudopotentials for the energy range of 2.0–40 eV and angular range of 0°–180°. The resemblance of the π^* shape resonance in the cross sections, observed at 1.5–2.0 eV for propene, to those in C₂H₄ and C₂F₄ clearly points to the effect of the double bond in the molecular structures for these molecules. Below 60 eV, we observed clear differences in peak positions and magnitudes between the DCS, ECS, and MTCS for C₃H₆ and *c*-C₃H₆, which we view as the isomer effect. © 2006 American Institute of Physics. [DOI: 10.1063/1.2141950]

I. INTRODUCTION

The industrial importance of hydrocarbons has been established over the last few years, since they play an important role in plasma diagnostics as impurities in the tokamak fusion divertor, as feed gases for production of radicals and ions in low-temperature plasma processing, and many other fields.¹ In particular, cyclopropane (hereafter referred to as *c*-C₃H₆) has been reported to constitute a significant proportion of the gaseous part of the cold edge fusion plasmas.² Besides, from a pure physical point of view, hydrocarbons can be classified into the groups alkanes, cycloalkanes, alkenes, and alkynes, which have different molecular structures that offer an interesting platform for studying electron-molecule scattering dynamics. Even more interesting is the study of electron collisions with an isomeric pair consisting of an alkane and its corresponding cycloalkane, as they have the same chemical properties and only differ in the molecular structure.

In this report the two stable isomers of C₃H₆ molecules, propene [H₃C–CH=CH₂] and cyclopropane [cyclic(H₂C–CH₂–CH₂)], are studied. *c*-C₃H₆ has only single bonds, whereas propene (hereafter referred to as

C₃H₆), just like ethylene (C₂H₄) and allene (C₃H₄), has a double bond C=C, offering a case study of resonances due to the presence of valence unoccupied orbitals with C=C antibonding character. However, though C₃H₄ has received relatively larger research attention (see, for example, Refs. 3–5 and references therein), electron cross-section data on C₃H₆ remain scarce and fragmentary to date. To our knowledge there exist no absolute differential cross sections (DCS), except for one theoretical study.⁶ However, there exist some experimental and theoretical electron-impact studies of other cross sections for these molecules worth mentioning. These include the earliest works on low-energy electronic excitation spectra obtained using the trapped-electron technique,⁷ ionization cross-section measurements,⁸ the electron swarm experiments for momentum transfer and vibrational excitation,⁹ and the measurements of energy-loss spectra.¹⁰ Works that later followed these include the electron-impact experimental^{11,12} and theoretical¹³ ionization cross-section (ICS) studies and experimental total cross sections (TCS).^{14–17} On the other hand, a much wider spectrum of works exists in literature on the individual *c*-C₃H₆ molecules, i.e., possibly owing to interests in its C–C–C ring structure, in addition to the combined studies with its isomer partner, i.e., the linear C₃H₆ molecule. These include the experimental^{16–18} and theoretical¹⁸ TCS and experimental¹¹

^{a)}Electronic mail: c-makoch@sophia.ac.jp

and theoretical¹³ ICS. In addition, Allan¹⁹ carried out extensive high-resolution work investigating the electron-impact vibrational excitation cross sections. In this study he also measured the electron affinity for the molecules. Quantum calculations were carried out too in the investigation of a number of the vibrational modes.²⁰ Elastic DCS for these molecules have been studied mainly theoretically,^{6,21,22} although there exists, to our knowledge, also one measurement.²³ High-resolution electron-energy-loss spectroscopy experiments were employed to study singlet-triplet, inner-shell, and valence-shell electronic excitations, of these molecules,^{24–26} while photoabsorption and photoelectron spectra were also studied and helped in establishing the electronic states for these molecules.^{27,28}

In this report we present results of a joint experimental and theoretical work on electron collisions with the C₃H₆ isomers. The energy ranges are from 1.5 to 100 eV and 2–40 eV, for the experimental and theoretical results, respectively. This work is a part of the systematic study on isomer molecules that we started with the study of the isomers of C₃H₄, allene, and propyne.^{5,29,30}

II. EXPERIMENTAL PROCEDURE

The apparatus used in the present DCS measurements is the same as that used in our previous studies.³¹ The overall energy resolution was 30–50 meV, while the angular resolution was $\pm 1.5^\circ$. Thus, the present DCS are considered to be the sum of the elastic process and the rotational excitation and deexcitation processes, although the vibrational levels are sufficiently discriminated. Absolute cross sections were obtained by the relative flow technique³² using helium as the reference gas. The electron energy scale was calibrated with respect to the 19.367 eV resonance for He. The DCS were analyzed using a molecular phase-shift approach³³ in order to extrapolate the DCS to lower and higher angles, i.e., $\theta < 20^\circ$ and $\theta > 130^\circ$, to facilitate derivation of the integral cross sections. Experimental errors in the DCS were estimated to be 10%–15%, whereas those in the derived integral elastic cross sections (ECS) and momentum-transfer cross sections (MTCS) were 20%–25%.

III. THEORETICAL PROCEDURE

To compute the ECS, DCS, and MTCS cross sections for C₃H₆ and *c*-C₃H₆, we employed the Schwinger multichannel method³⁴ (SMC) with pseudopotentials.³⁵ Since the SMC method has been described in detail in several publications, we will only describe here those points directly concerned with the calculations for this present paper. For each one of these C₃H₆ isomers, our calculations (bound state and scattering) were performed using the experimental equilibrium geometry of the molecular ground state from Ref. 36. The basis set used in the present calculations is the same as that used in Ref. 29, except for the point that we have not included the *p*-type function for the hydrogen. Our scattering calculations were performed using the static exchange and static exchange plus polarization approximations. Nuclear motion was not allowed in the present calculations. To include polarization effects, we enlarged our configuration

space to include configuration state functions (CSFs) generated through virtual excitations of the molecular target as described in Ref. 37.

Propene belongs to the C_s group and has a small permanent dipole. In the calculation of the DCS for energies up to 5 eV, we have included the long-range interaction through the first Born approximation of the dipole potential. For C₃H₆, our calculated values for the dipole moment and for the polarizability are 0.385 D and 6.73×10^{-30} cm³, respectively. These calculated values are in good agreement with the experimental values of 0.366 D and 6.26×10^{-30} cm³ for the dipole moment and for the polarizability, respectively.³⁶ The number of CSFs by symmetry included in our calculations was 4213 CSFs for A' and 1746 CSFs for A'', giving a total of 5959 CSFs for the entire calculation. For the A'' symmetry, which is resonant in nature, we considered only excitations from the occupied orbitals to the virtual orbitals which preserved the spatial symmetry of the ground state, and all singlet- and triplet-coupled single excitations were included. To represent the scattering orbital we used only one modified virtual orbital.^{38,39}

Cyclopropane belongs to the D_{3h} group, but due to symmetry reasons our calculations were performed in the C_{2v} group. Our calculated value of 5.79×10^{-30} cm³ for the polarizability agrees well with the experimental value of 5.66×10^{-30} cm³. The number of CSFs by symmetry included in our calculations was 3959 for A₁, 3911 for B₁, 2333 for B₂, and 2296 for A₂, giving a total of 12 489 CSFs for the entire calculation.

It is worth pointing out that, of the results available in literature, the data of Winstead *et al.*⁶ were also obtained with the Schwinger multichannel method. However, they completely neglected polarization effects, since the calculations were performed at the static-exchange approximation, and also employed a smaller basis set. Another difference between the two calculations is that we used pseudopotentials to replace the core electrons, i.e., only the valence electrons are taken into account in our calculations. In contrast, the calculations of Winstead *et al.* considered all electrons.

IV. RESULTS AND DISCUSSION

The order of the discussion is as follows. The DCS results for each individual molecule are discussed first. This is followed by the discussion of the ECS and MTCS, the comparative study of the ECS with the TCS, and lastly the discussion of the isomer effect in these cross sections. The experimental cross sections are presented in Tables I–IV.

A. Propene

1. Differential cross sections (DCS)

Figure 1(a)–1(c) show a comparison between the current experimental and theoretical DCS results. For energies from 2 to 10 eV our calculated DCS were obtained at the static exchange plus polarization approximation, while those for energies above 10 eV were obtained at the static-exchange approximation. The only other results available, by Winstead *et al.*,⁶ are also included in the graphs for comparison over the energy range of overlap. The current experimental and

TABLE I. Electron-impact DCS (10^{-16} cm²/sr) for elastic scattering from propene (C₃H₆). The absolute uncertainties are $\pm 15\%$. The experimental integral cross section (ECS) and momentum-transfer cross section (MTCS) have units of 10^{-16} cm² and estimated to have experimental uncertainties of between 20% and 25%.

Angle (degrees)	1.5 eV	1.8 eV	2.0 eV	2.3 eV	2.6 eV	3.0 eV	5.0 eV
15	2.806	20.354
20	10.691	2.093	3.001	2.939	2.628	2.577	10.916
30	2.279	1.505	2.416	2.610	2.685	2.307	3.979
40	1.507	1.338	1.953	2.434	2.626	2.393	2.949
50	1.261	1.349	1.823	2.501	2.688	2.456	2.968
60	1.605	1.676	1.914	2.619	2.722	2.539	2.803
70	1.925	2.151	2.126	2.365	2.497	2.307	2.350
80	2.729	2.496	2.293	2.038	2.122	1.854	1.969
90	2.730	2.385	2.047	1.972	1.858	1.620	1.627
100	2.536	2.074	1.791	1.526	1.712	1.363	1.442
110	2.231	1.773	1.414	1.520	1.504	1.192	1.570
120	2.005	1.460	1.299	1.464	1.447	1.095	1.601
130	1.649	1.355	1.354	1.544	1.483	1.101	1.356
ECS	20.9	22.8	28.8	25.7	26.8	20.9	25.6
MTCS	21.5	21.8	25.8	22.4	24.4	18.9	20.4

theoretical results show plausible agreement both qualitatively and quantitatively, except for the lower-angle scattering for energies 2 and 3 eV. These energies are close to the shape resonance, and since our calculations have not included the nuclear motion, some differences between the theory and experiment are expected to occur. Some interesting features are observed and summarized as follows. (i) The 1.5–2.0 eV DCS show an angular dependence with a rising trend towards 0°. This rising trend towards 0° for these lower energies is expected for C₃H₆ as a result of enhanced forward scattering due to the presence of the dipole moment (0.366 D) and the relatively large polarizability (6.26×10^{-30} m³). (ii) The DCS for these three energies rise to produce the peaklike structure above 80°, which is consistent with the peak observed in both the ECS and TCS at around 2.2 eV (see Fig. 3). This DCS angular distribution is a characteristic of the *d*-wave scattering. (iii) These DCS show two shallow minima, a forward angle one centered at about 50°

(at 1.5 eV) that can be seen drifting towards 0° until it disappears at 2.3 eV (graph not shown). However, another one at the higher angle of about 110° is seen setting in at 2.0 eV and develops by drifting towards lower angles with increasing impact energy as well until it goes out of sight at 3.0 eV, as another one sets in again at the same energy at about 120°. (iv) Beyond 8.0 eV, however, the DCS show less structured angular dependence behavior, i.e., rather showing the same exponential decay pattern with pronounced minima in the region 60°–110°. This pattern of DCS over this energy range is consistent with the monotonic decrease seen in the ECS of Fig. 3.

In Figs. 1(a)–1(c) we also compare our current experimental and theoretical results with the only available theoretical data of Winstead *et al.* The agreement between the two theoretical results is fairly good over all the energies of overlap. As for the comparison between the Winstead *et al.* result and experiment, at 5.0 eV the agreement between the

TABLE II. Electron-impact DCS (10^{-16} cm²/sr) for elastic scattering from propene (C₃H₆). The absolute uncertainties are $\pm 15\%$. The ECS and MTCS have units of 10^{-16} cm² and estimated to have experimental uncertainties of between 20% and 25%.

Angle (degrees)	8 eV	10 eV	20 eV	30 eV	60 eV	100 eV
15	9.643	19.854	19.754	18.770	9.366	4.330
20	10.192	13.958	12.637	9.885	3.622	2.054
30	6.888	8.342	4.756	2.921	1.476	0.843
40	4.202	3.654	2.037	1.481	0.699	0.377
50	2.537	2.476	1.389	1.098	0.422	0.225
60	2.267	1.888	1.049	0.697	0.302	0.193
70	1.799	1.211	0.686	0.330	0.181	0.088
90	1.458	1.244	0.604	0.274	0.181	0.083
100	1.539	1.218	0.558	0.247	0.157	0.098
110	1.512	1.405	0.511	0.277	0.169	0.097
120	1.413	1.103	0.599	0.438	0.185	0.098
130	1.472	1.298	0.723	0.452	0.235	0.101
ECS	28.6	33.5	25.1	19.8	11.6	6.1
MTCS	19.9	19.1	13.7	8.9	8.1	4.3

TABLE III. Electron-impact DCS (10^{-16} cm²/sr) for elastic scattering from cyclopropane (*c*-C₃H₆). The absolute uncertainties are $\pm 15\%$. The ECS and MTCS have units of 10^{-16} cm² and estimated to have experimental uncertainties of between 20% and 25%.

Angle (degrees)	1.5 eV	2.0 eV	3.0 eV	4.0 eV	5.0 eV	7.0 eV	10.0 eV
20	1.920	2.233	3.132	4.859	8.545	9.555	11.57
30	1.206	1.214	1.513	2.331	4.287	4.874	5.81
40	0.729	0.944	1.243	1.784	2.538	2.854	2.806
50	0.727	0.927	1.124	1.746	2.221	2.348	1.949
60	0.878	1.068	1.148	1.681	2.145	2.131	1.722
70	1.084	1.220	1.195	1.495	1.723	1.688	1.398
80	1.353	1.394	1.234	1.094	0.978	0.993	0.973
90	1.479	1.487	1.121	0.827	0.732	0.851	0.924
100	1.601	1.481	1.036	0.863	1.145	1.283	1.386
110	1.645	1.258	1.032	1.096	1.837	2.099	1.964
120	1.621	1.201	1.216	1.312	2.279	2.374	2.085
130	1.622	1.203	1.361	1.465	2.645	2.145	1.682
ECS	17.7	17.2	17.8	19.5	28.9	30.8	30
MTCS	19.1	17.6	17.1	18.5	26.4	24.7	21.3

two is not good below 60°, where their result stays on a plateau whereas ours is showing a rising trend with decreasing energy. Above 60° degrees, however, the two results show good agreement. The agreement at the three impact energies of 8, 10, and 20 eV is very good over all the range of scattering angles of overlap. At 30 eV, however, although the two theoretical results agree well over the whole range of scattering angles, the agreement with experiment is not good at 60°–120°, where the experimental result shows a minimum, whereas the two theories are rather flat.

2. Elastic integral cross section (ECS) and momentum-transfer cross section (MTCS)

Figures 2(a) and 2(b) show the current experimentally derived and theoretical ECS and MTCS results, respectively. Also shown in both figures are the previous results by other groups. For energies 1–15 eV, our calculated ECS and MTCS were obtained at the static exchange plus polarization ap-

proximation, while for energies above 15 eV we used the static-exchange approximation. The comparison between both our current experimental and theoretical results with the result of Winstead *et al.*⁶ is generally good both qualitatively and quantitatively above 10 eV. However, their ECS data shows a minimum at about 8 eV, before showing a turn for the rise, contrary to our two data sets. Nearly the same pattern of differences is observed again in the comparison of our experimentally derived MTCS result with theirs, i.e., with their result showing a sharp decrease below 9 eV. In view of the differences observed in the current two data sets for MTCS with those of Winstead *et al.*, we tried switching their MTCS result for C₃H₆ with that for *c*-C₃H₆ and found a surprising similarity with our two data sets. We thus point out that we suspect that Winstead *et al.*⁶ might have possibly mistakenly switched labels in naming their MTCS curves in Fig. 5 of their paper.

In Fig. 3 we show both the current experimental and

TABLE IV. Electron-impact DCS (10^{-16} cm²/sr) for elastic scattering from cyclopropane (*c*-C₃H₆). The absolute uncertainties are $\pm 15\%$. The ECS and MTCS have units of 10^{-16} cm² and estimated to have experimental uncertainties of between 20% and 25%.

Angle (degrees)	12 eV	15 eV	20 eV	25 eV	30 eV	60 eV	100 eV
15	15.74	16.853	18.37	20.086	22.44	15.34	9.1
20	11.73	12.453	12.98	12.407	12.27	6.46	3.068
30	5.784	5.898	4.963	4.026	3.5	1.22	0.774
40	2.581	2.355	1.908	1.645	1.444	0.673	0.358
50	1.661	1.53	1.354	1.277	1.061	0.368	0.252
60	1.587	1.451	1.243	0.971	0.736	0.258	0.189
70	1.411	1.275	0.924	0.644	0.442	0.223	0.103
80	1.051	0.944	0.644	0.457	0.357	0.1469	0.063
90	0.934	0.858	0.581	0.458	0.391	0.094	0.056
100	1.22	0.95	0.663	0.518	0.484	0.0846	0.074
110	1.52	1.09	0.718	0.53	0.522	0.106	0.076
120	1.634	1.13	0.812	0.61	0.644	0.142	0.094
130	1.334	1.035	0.851	0.674	0.863	0.18	0.115
ECS	28	27.2	25.5	23.8	22.6	11.8	6.4
MTCS	17.7	15.4	11.5	10.6	9.8	8.6	4.7

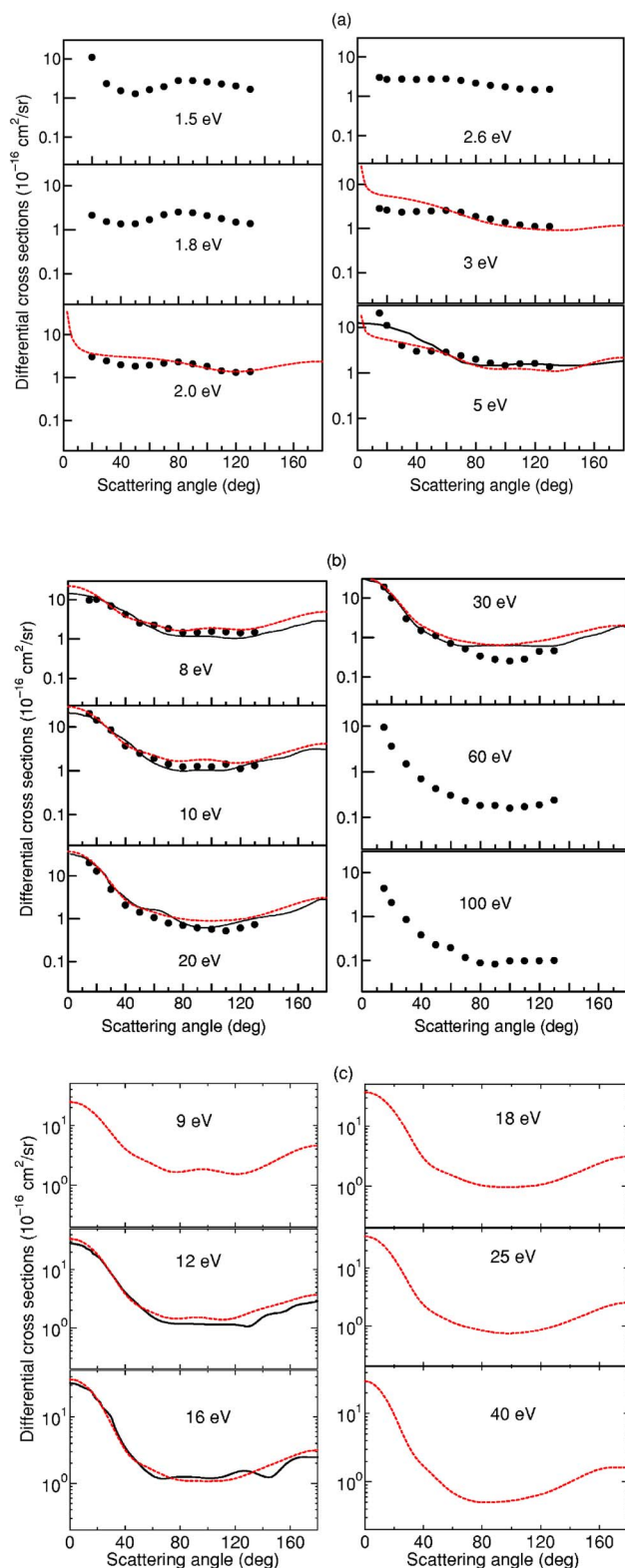


FIG. 1. Present electron-impact C₃H₆ experimental (circles) and theoretical (red dashed lines) DCS as functions of the scattering angles. Also included in some panels are the only available DCS results of Winstead *et al.* (Ref. 6) (black solid lines), for comparison at the energies of overlap.

theoretical ECS in comparison with the grand TCS by this group⁴⁰ and those by Szymkowski and Kwitnewski,¹⁷ i.e., the largest of all in magnitude amongst the three results available in literature.^{15–17} The ECS results reproduce well the structures observed in the TCS above 1 eV, although the

experimental results involve rather large errors. That is, the 2.2 eV and the 9.5 eV resonance peaks before decreasing monotonously. It is worth pointing out that the 2.2 eV peak, which by the current calculations is assigned to the A' symmetry, should be attributable to the phenomenon observed to be characteristic of all C=C double bond containing hydrocarbons. The phenomenon involves a temporary trapping of the incoming electron into valence orbitals with the C=C antibonding character, i.e., the lowest unoccupied molecular orbital (LUMO) of that symmetry, which is a π^* -shape resonance.⁶ In the elastic scattering channel, however, elastic scattering via resonances is in general smeared out by the direct elastic component. Nevertheless, these resonances can in most cases be clearly revealed in vibrational excitation functions by experiments that sweep impact energies across the resonance region. The resonance peak at about 9.5 eV should be attributable to a shape resonance of the A₁ symmetry type that has been observed as characteristic of hydrocarbons in this region. Contributions from other several inelastic scattering processes, e.g., vibrational excitation, should also be significant.^{7,8,40} The current calculations further show that this broad structure around 9.5 eV belongs to the A' symmetry.

As expected, the difference between the ECS and the TCS increases above 20 eV owing to the growing significance of the inelastic channels, mainly the ionization channel. The ionization channel, for instance, has a threshold at 9.73 eV and rises to a peak at about 100 eV, where it overtakes the ECS in magnitude (see Fig. 3). Above this ionization threshold, the combination of the elastic and ionization channels is expected to form more than 90% of the TCS. Our TCS is greater than the sum of our ECS plus the ICS by Nishimura and Tawara¹¹ by 9.9% at 30 eV and 9.8% at 100 eV. Compared to this, the data of Szymkowski and Kwitnewski¹⁷ are, respectively, 27.5% and 38.3% greater than this ECS and ICS sum, which indicates a possible overestimation of their TCS magnitudes.

B. Cyclopropane

1. DCS

The current experimental and theoretical results are presented Figs. 4(a)–4(r). For energies 2–10 eV, our calculated DCS include polarization effects, while for energies above 10 eV they were obtained at the static-exchange approximation. Where available, results from literature have also been drawn into the panels for the various energies of overlap. The agreement between our experimental and theoretical result is not good below 5 eV. At 5 eV, though the qualitative agreement is good between 30°–120°, the theoretical result is clearly underestimating the DCS at forward scattering angles towards 0°. However, at this region, the current theoretical result seems to agree well with the other theoretical results by Winstead *et al.*⁶ (both calculations done with the SMC method) and Beyer *et al.*,²¹ whereas the two experimental results agree between themselves, as well as with the theoretical result by Curik and Gianturco.²² In the SMC method, the scattering wave function is expanded in a basis set formed by square integrable functions (L^2 functions); the

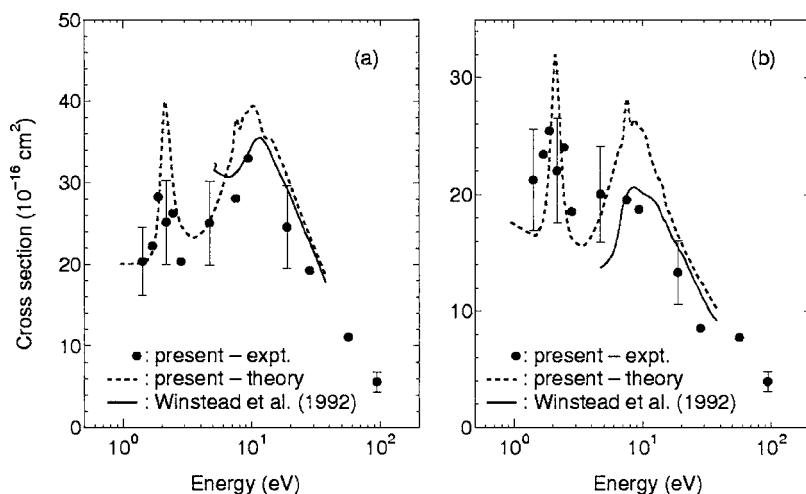


FIG. 2. (a) ECS: present experimental and theoretical results compared with those by Winstead *et al.* (Ref. 6), and (b) MTCS: present experimental results compared with those by Winstead *et al.* (Ref. 6).

scattering wave function does not need to satisfy any boundary condition, which is incorporated in the Green's function. The discrepancy seen between the present theory and the experiment between 2 and 5 eV may be due to the fact that the SMC method, due to its L^2 character, fails in the description of higher partial waves, since this occurs mostly at low scattering angles. This does not occur with the results of Curik and Gianturco (who use a single center expansion, and are thus able to account for the higher partial waves), which agree with the experiment at all angles of overlap. However, the current experimental and theoretical results are found to agree well both qualitatively and quantitatively at overlapping energies at 7 eV and above with all three theoretical^{6,21,22} and one experimental result.²³

These results are summarized as follows. (i) The 1.5–15 eV impact energy range is characterized by DCS showing a very wavy structure. (ii) The rising DCS towards 0° at 4 eV and below can be associated with the relatively larger polarizability of these molecules, $5.66 \times 10^{-30} \text{ m}^3$, resulting in enhanced scattering at the forward scattering angles. (iii) The 70° – 120° DCS for energies 1.5–2.0 eV show peaks typically associated with resonance peaks in the TCS. This peak seems

to be increasing in magnitude with decreasing impact energies below 2 eV, a fingerprint of a low-lying resonance at about 1.5 eV, or below [see Fig. 5(a)]. Indeed, the TCS results of our group⁴⁰ show a weak shoulder, reminiscent of a weak resonance feature centered at about 1.5 eV, in agreement with the current DCS and ECS features (see Fig. 6). On the contrary, the result obtained by Szymtkowski and Kwitniewski¹⁷ shows a much broader peak shoulder centered at about 2.6 eV. We do not find any evidence for such a feature, i.e., neither in the current DCS and ECS nor in our vibrational excitation cross sections.⁴⁰ However, this weak feature at 1.5 eV in the TCS is not solely due to the elastic channel but should also be made up of some contributions from both the C–C ring deformation (ν_{11}) and symmetric ring stretching (ν_3) vibrational excitation, which exhibit weakly rising excitation functions below 2 eV.¹⁹ (iv) The DCS for energies 1.5–10 eV show two minima, i.e., one at the forward angle of 50° and another at a higher angle of about 110° . These minima can be seen moving towards lower angles. It is also clear that these DCS have also developed a higher-angle peak that is deeper and appears at about 120° at 10 eV. (v) Beyond 10 eV, the angular distributions of the DCS are not spectacular, as they just show smooth variation with increasing angles.

2. ECS and MTCS

Figures 5(a) and 5(b) show the current experimental and theoretical ECS and MTCS results, respectively. Also shown in these graphs are the results by Winstead *et al.*,⁶ Beyer *et al.*,²¹ and Curik and Gianturco.²² The agreement of the ECS with these literature results is good qualitatively, except for a few eV shift in the main resonance peak position: about 7.5 eV for this experimental work, 13 eV for Curik and Gianturco, and 9 eV for Winstead *et al.* As for the MTCS, the agreement is good above 13 eV, both qualitatively and quantitatively. However, below this energy, the current result shows a peak at about 4.5 eV while the MTCS obtained by Winstead *et al.* shows a peak at about 11 eV. In addition, though both MTCS results show low-energy minima, ours is located at 3 eV, whereas their result shows a minimum at 6 eV. Although the calculations of Curik and Gianturco give DCS which agrees very well with the experiment, they seem

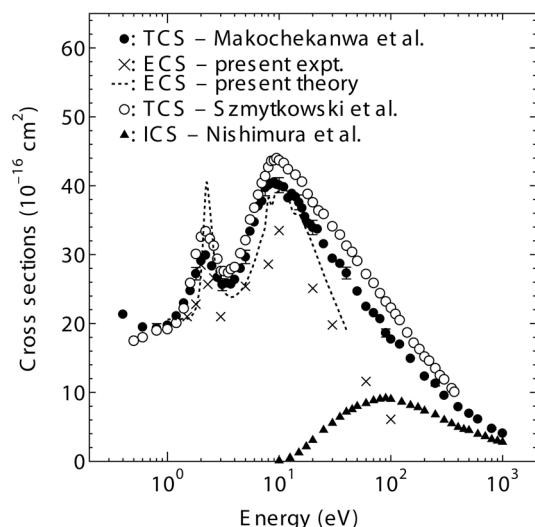


FIG. 3. Present C_3H_6 experimental and theoretical ECS results compared with the TCS by our group (Ref. 40), those of Szymtkowski *et al.* (Ref. 17), and the ICS results of Nishimura *et al.* (Ref. 11).

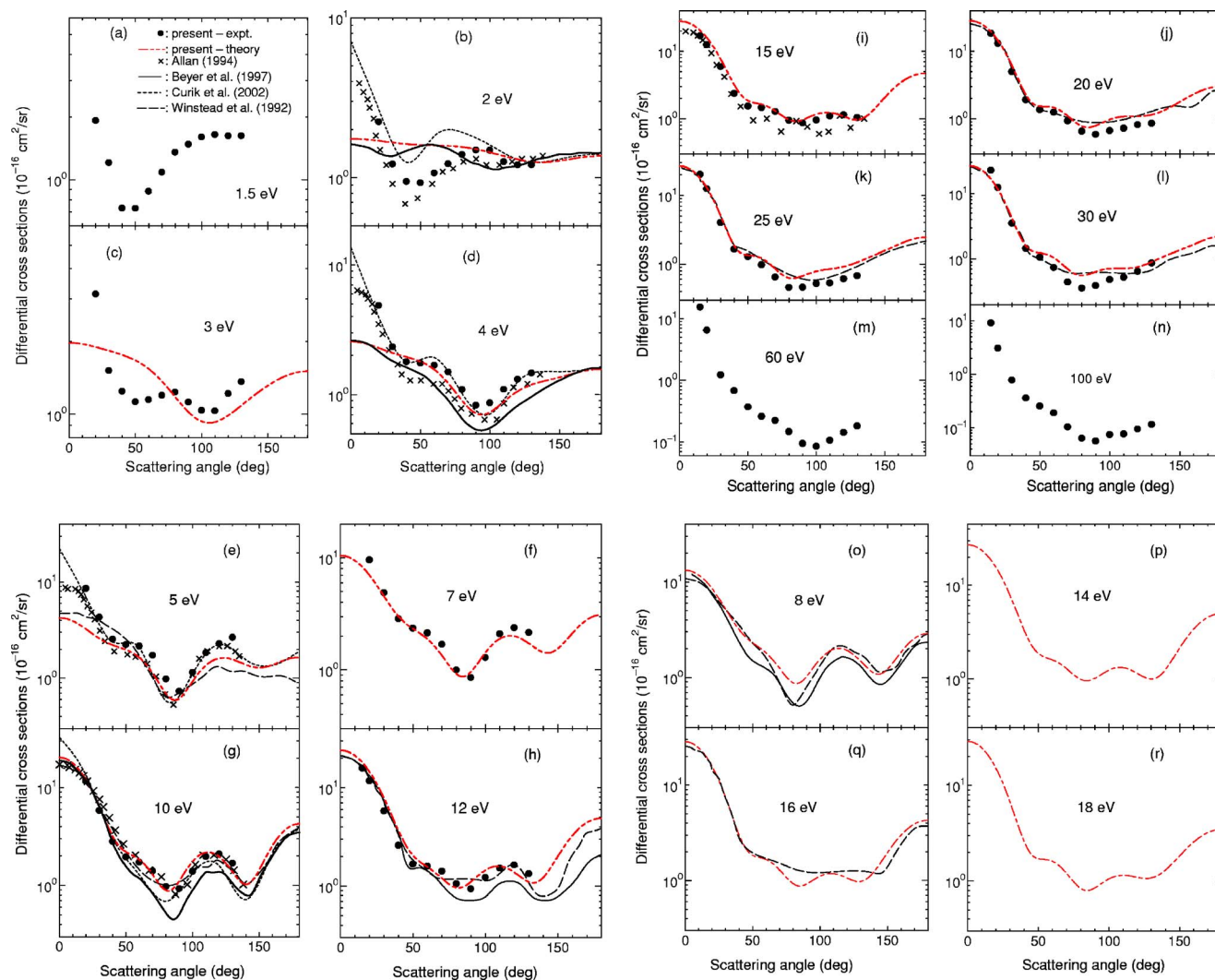


FIG. 4. Present DCS compared with the available results from literature. In Fig. 4(e), the results of Allan (Ref. 23) and Curik *et al.* (Ref. 22) shown for comparison with our 5 eV data are the data for 5.5 eV.

to overestimate the ECS. See our comment above in the C₃H₆ MTCS discussion on these differences between our MTCS and those of Winstead *et al.*

As shown in Fig. 6, these experimental and theoretical ECS results reproduce the structures observed in the TCS in general, albeit with the experimental ECS showing better

results. However, it is worth pointing out that although the theoretical ECS reproduce this weak feature at about 1.5 eV in the TCS obtained by our group, it overestimates the magnitudes, i.e., being greater than both TCS sets shown in Fig. 6 below 1.5 eV. Below about 6 eV, it can be clearly seen that the TCS is mainly made up of the elastic channel. The near

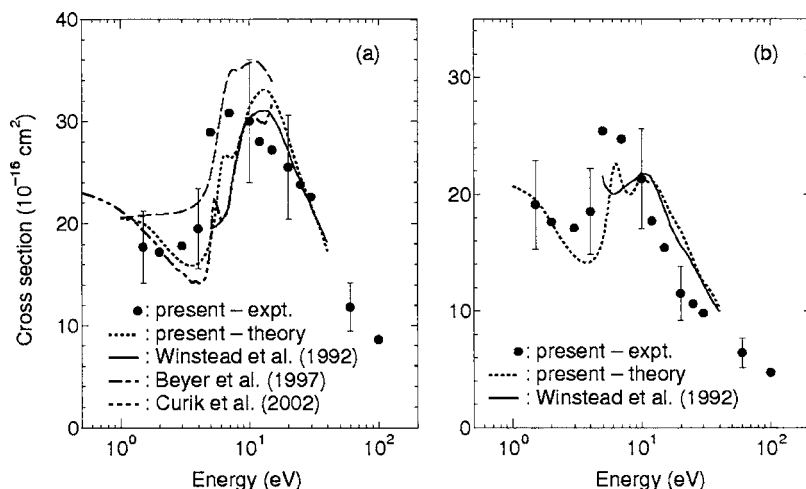


FIG. 5. (a) ECS: present experimental and theoretical results compared with those by other groups, and (b) MTCS: present experimental results compared with those by Winstead *et al.* (Ref. 6).

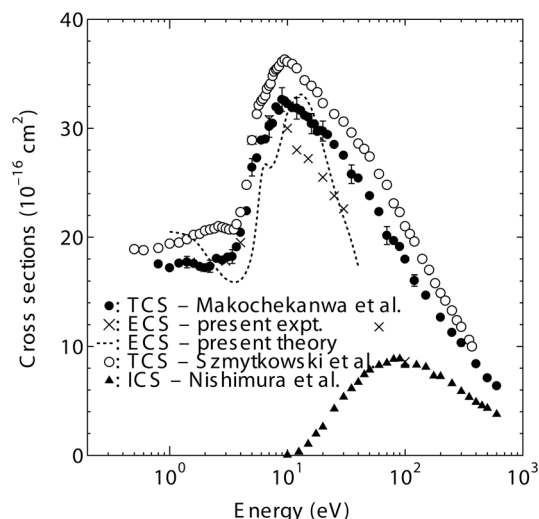


FIG. 6. Present c - C_3H_6 experimental and theoretical ECS results compared with the TCS by our group (Ref. 40), those of Szymtkowski *et al.* (Ref. 17), and the ICS results of Nishimura *et al.* (Ref. 11).

equal TCS and ECS results agree well with our observation that the vibrational excitation cross sections are very small;⁴⁰ thus also pointing out to the fact that there is no other significant channel contributing to the TCS at this lower-energy range. A change of slope is clearly observable in both TCS data sets and the two sets of ECS at about 6 eV. This is attributable to the A'_2 shape resonance discussed by Winstead *et al.*⁶ According to our calculations, this shape resonance is located around 6.2 eV, i.e., in agreement with the results of Curik and Gianturco.²² The calculations of Beyer *et al.*²¹ place this resonance around 5.4 eV. According to the experimental ECS result, the difference between the TCS and ECS data starts to emerge above 7 eV, as expected from the opening up of the electronic excitation channel, before the main peak centered at about 9.5 eV. This 9.5 eV peak has an origin similar to that observed in the C_3H_6 , i.e., a typical shape resonance peak common to all hydrocarbons. This main broad peak in the TCS is also seen in the calculated ECS. In our calculations, as in the calculations of Beyer *et al.* and Curik and Gianturco, there is a broad structure belonging to the E' symmetry around this energy. It is also clearly visible that as the ECS decrease beyond the main peak at about 9.5 eV, the ICS channel becomes the dominant contributor to the TCS, constituting about 50% of the TCS. However, once again the unexpectedly large difference between our current ECS results and the largest grand TCS available in literature, i.e., that of Szymtkowski *et al.*,¹⁷ prompted us to plot Fig. 6. Again we carry out a rough cross-section magnitude inspection by examining the difference between the sum of the current experimental ECS and the ICS of Nishimura *et al.*¹¹ Above the ionization threshold, these two channels should almost equal the TCS, except for the contribution from the electronic excitation channel. The result is that the sum is less than the TCS obtained by our group by 6%, against 19.8% of Szymtkowski and Kwitniewski, and 6% against 16%, at 10 eV and 100 eV, respectively.

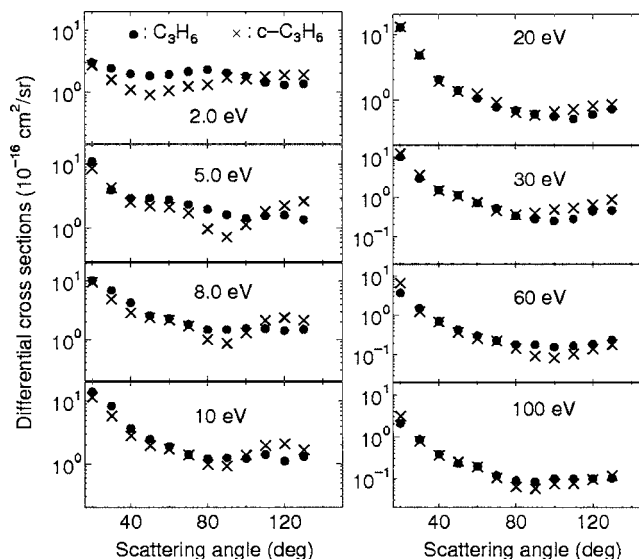


FIG. 7. C_3H_6 and c - C_3H_6 electron-impact DCS for selected energies.

C. On the isomer effect between C_3H_6 and c - C_3H_6 : DCS and ECS

Figure 7 shows the experimental DCS for these two molecules for the selected energies of 2, 5, 8, 10, 20, 30, 60, and 100 eV. Isomer effects are observed at low energies but become less pronounced for energies 60 eV and above. At energies below 10 eV, where polarization effects are more important, the phenomenon can be explained as due to different polarizabilities of these molecular targets. This can give rise to distinct overall scattering potentials and account for the isomer effects. At intermediate energies the phenomenon can have its origin in multichannel coupling (different electronic excitation and ionization spectra) and/or interference effects. Considering that the isomer effects are seen in the present theoretical results, where multichannel coupling is not taken into account, possible differences in the multichannel coupling of the two molecules cannot be the only origin for these effects. Interference effects are related to molecular geometry and are due to the wave character of the electron. The electron is scattered by different portions of the target and has constructive or destructive chances to be collected by the detector. These effects are clearly seen in electron-atom collisions where the DCS always present large structures (deep minima). On the molecular case, due to the presence of randomly oriented molecules in a gaseous target, the interference structures can (angularly) move around according to the orientation of the molecule, resulting in averaged smoother DCS than in the atomic case. Molecules with higher geometric symmetries can preserve interference effects when scattered by electrons from different orientations. This phenomenon can be noticed in Fig. 7 where c - C_3H_6 shows more pronounced dips for most of the energies studied than C_3H_6 .

A comparison between the calculated ECS for the two C_3H_6 isomers shows that large differences between the isomers cross sections are seen below 20 eV. These differences allow one to distinguish between the two isomeric cross sections. For energies between 20 and 60 eV the differences are

still noticeable, although they become smaller. The ECS converge for energies above 60 eV. In this case the isomer effect occurs for energies below 60 eV. The same behavior is seen in the MTCS.

V. CONCLUSIONS

In this paper experimental and theoretical electron-impact elastic integral, differential and momentum transfer cross sections have been studied for the energy ranging from 1.5 to 100 eV and 2.0 and 40 eV, respectively. In the case of C₃H₆, good agreement was obtained between the current experimental and theoretical results over all energies and all scattering angles of overlap. For *c*-C₃H₆, however, although good agreement was observed at energies 7 eV and above, discrepancies were observed at lower energies. The DCS for C₃H₆, for energies 1.5–5 eV, show angular distributions characterized by a set of lower-angle and higher-angle minima, whereas the DCS for 8 eV and above show monotonously decaying profiles. For *c*-C₃H₆, the 1.5–7 eV impact energy range is characterized by DCS showing very wavy structures, whereas the DCS for the higher energy range show smooth decay curves. We observed clear differences in peak positions and magnitudes between the DCS for C₃H₆ and *c*-C₃H₆, which we view as the isomer effect.

Our calculated ECS for C₃H₆ show a shape resonance located around 2.2 eV, which agrees with both the experimental ECS and the TCS positions and has been assigned to the A'' symmetry of the C_s group. For *c*-C₃H₆, our calculated ECS show a shape resonance located at around 6.2 eV and belonging to the A'₂ symmetry of the D_{3h} group. This resonance in *c*-C₃H₆ has been observed in other calculations by other groups before. In the comparison between the ECS results for these two molecules, the isomer effect is found to occur for energies below 60 eV.

ACKNOWLEDGMENTS

This work was supported in part by a Grant-in-Aid from the Ministry of Education, Science, Technology, Sport, and Culture, Japan; the Japan Society for the Promotion of Science (JSPS); and the Japan Atomic Energy Research Institute (JAERI). One of the authors (C.M.) is also grateful to the JSPS for financial support under Grant No. P04064. Another author (H. Kubo) acknowledges Dr. T. Ozeki of the JAERI for his encouragement and support during this work. This work was also done under the International Atomic Energy Agency (IAEA) project of three of the authors (C.M., M.H., and H.T.). Another three authors (M.H.F.B., M.A.P.L., and L.G.F.) acknowledge support from the Brazilian agency Conselho Nacional de Desenvolvimento Científico e Tecnológico (CNPq). One author (M.H.F.B.) also acknowledges Professor Carlos M. de Carvalho for computation support at Departamento de Física-UFPR and support from the Paraná state agency Fundação Araucária and from the FINEP (under Project No. CT-Infra 1). One author (A.R.L.) acknowledges support from the FAPESP. These calculations were made at CENAPAD-SP and at DF-UFPR.

- ¹W. L. Morgan, *Adv. At., Mol., Opt. Phys.* **43**, 79 (2000).
- ²H. Tawara, Y. Itikawa, H. Nishimura, H. Tanaka, and Y. Nakamura, National Institute for Fusion Science Report No. NIFS-DATQA-6, 1990. (unpublished)
- ³L. D. Hulett, D. L. Donohue, J. Xu, T. A. Lewis, S. A. McLuckey, and G. L. Glish, *Chem. Phys. Lett.* **216**, 236 (1993).
- ⁴R. Panajotovic, M. Jelisavcic, R. Kajita, T. Tanaka, M. Kitajima, H. Cho, H. Tanaka, and S. J. Buckman, *J. Chem. Phys.* **121**, 4559 (2004).
- ⁵C. Makochekanwa, H. Kawate, O. Sueoka, M. Kimura, M. Kitajima, M. Hoshino, and H. Tanaka, *Chem. Phys. Lett.* **368**, 82 (2003).
- ⁶C. Winstead, Q. Sun, and V. McKoy, *J. Chem. Phys.* **96**, 4246 (1992).
- ⁷C. R. Bowman and W. D. Miller, *J. Chem. Phys.* **42**, 681 (1965).
- ⁸B. L. Schram, M. J. van der Wiel, F. J. de Heer, and H. R. Moustafa, *J. Chem. Phys.* **44**, 49 (1966).
- ⁹C. W. Duncan and I. C. Walker, *J. Chem. Soc., Faraday Trans. 2* **70**, 577 (1974).
- ¹⁰K. E. Johnson, D. B. Johnston, and S. Lipsky, *J. Chem. Phys.* **70**, 3844 (1979).
- ¹¹H. Nishimura and H. Tawara, *J. Phys. B* **27**, 2063 (1994).
- ¹²D. Lukic, G. Josifov, and M. V. Kurepa, *Int. J. Mass. Spectrom.* **205**, 1 (2001).
- ¹³H. Deutsch, K. Becker, R. K. Janev, M. Probst, and T. D. Mark, *J. Phys. B* **33**, L865 (2000).
- ¹⁴S. L. Lunt, J. Randell, J.-P. Ziesel, G. Mrozek, and D. Field, *J. Phys. B* **31**, 4225 (1998).
- ¹⁵K. Floeder, D. Fromme, W. Raith, A. Schwab, and G. Sinapius, *J. Phys. B* **18**, 3347 (1985).
- ¹⁶H. Nishimura and H. Tawara, *J. Phys. B* **24**, L363 (1991).
- ¹⁷C. Szmytkowski and S. Kwitniewski, *J. Phys. B* **35**, 2613 (2002).
- ¹⁸Y. Jiang, J. Sun, and L. Wan, *Phys. Rev. A* **62**, 062712 (2000).
- ¹⁹M. Allan, *J. Am. Chem. Soc.* **115**, 6418 (1993).
- ²⁰R. Curik and F. Gianturco, *J. Phys. B* **35**, 1235 (2002).
- ²¹T. Beyer, B. M. Nestmann, B. K. Sarpal, and S. D. Peyerimhoff, *J. Phys. B* **30**, 3431 (1997).
- ²²R. Curik and F. Gianturco, *J. Phys. B* **35**, 717 (2002).
- ²³M. Allan, in *Electron Collisions with Molecules, Clusters, and Surfaces*, edited by H. Ehrhardt and L. A. Morgan (Plenum, New York, 1994).
- ²⁴K. H. Sze and C. E. Brion, *J. Electron Spectrosc. Relat. Phenom.* **57**, 117 (1991).
- ²⁵H. H. Brongersma and L. J. Oosterhoff, *Chem. Phys. Lett.* **3**, 437 (1969).
- ²⁶M. P. Banjavcic, T. A. Daniels, and K. T. Leung, *Chem. Phys.* **155**, 309 (1991).
- ²⁷H. Koizumi, T. Yoshimi, K. Shinsaka, M. Ukai, M. Morita, Y. Hatano, A. Yagishita, and K. Ito, *J. Chem. Phys.* **82**, 4856 (1985).
- ²⁸H. Basch, M. B. Robin, N. A. Kuebler, C. Baker, and D. W. Turner, *J. Chem. Phys.* **51**, 52 (1969).
- ²⁹S. d'A. Sanchez, A. R. Lopes, M. H. F. Bettega, M. A. P. Lima, and L. G. Ferreira, *Phys. Rev. A* **71**, 062702 (2005).
- ³⁰Y. Nakano, M. Hoshino, M. Kitajima, H. Tanaka, and M. Kimura, *Phys. Rev. A* **66**, 032714 (2002).
- ³¹H. Tanaka, T. Ishikawa, M. Masai, T. Sagara, L. Boesten, M. Takekawa, Y. Itikawa, and M. Kimura, *Phys. Rev. A* **57**, 1798 (1998).
- ³²S. K. Srivastava, A. Chutjian, and S. Trajmar, *J. Chem. Phys.* **63**, 2659 (1975).
- ³³R. Panajotovic, M. Kitajima, H. Tanaka, M. Jelisavcic, J. Lower, L. Campbell, M. J. Brunger, and S. J. Buckman, *J. Phys. B* **36**, 1615 (2003).
- ³⁴K. Takatsuka and V. McKoy, *Phys. Rev. A* **24**, 2473 (1981); **30**, 1734 (1984).
- ³⁵M. H. F. Bettega, L. G. Ferreira, and M. A. P. Lima, *Phys. Rev. A* **47**, 1111 (1993).
- ³⁶*CRC Handbook of Chemistry and Physics*, 79th ed., edited by D. R. Lide (CRC, Boca Raton, 1998).
- ³⁷T. N. Rescigno, C. W. McCurdy, and B. I. Schneider, *Phys. Rev. Lett.* **63**, 248 (1989).
- ³⁸C. W. Bauschlicher, *J. Chem. Phys.* **72**, 880 (1980).
- ³⁹C. Winstead and V. McKoy, *Phys. Rev. A* **57**, 3589 (1998).
- ⁴⁰C. Makochekanwa, H. Kato, M. Hoshino, H. Cho, M. Kimura, O. Sueoka, and H. Tanaka, *Eur. Phys. J. D* **35**, 249 (2005).